

## An Eclipsing Black Widow Pulsar in NGC 6712

ZHEN YAN,<sup>1,2,3</sup> ZHI-CHEN PAN,<sup>4,5</sup> SCOTT M. RANSOM,<sup>6</sup> DUNCAN R. LORIMER,<sup>7,8</sup> LEI QIAN,<sup>4,5</sup> PEI WANG,<sup>4,5</sup>  
ZHI-QIANG SHEN,<sup>1,2,3</sup> DI LI,<sup>2,4,5</sup> PENG JIANG,<sup>2,4,5</sup> JIN-TAO LUO,<sup>2,9</sup> JIE LIU,<sup>1,2</sup> AND ZHI-PENG HUANG<sup>1,2</sup><sup>1</sup>*Shanghai Astronomical Observatory, Chinese Academy of Sciences, NO. 80 Nandan Road, Shanghai 200030, China*<sup>2</sup>*University of Chinese Academy of Sciences, No.19A Yuquan Road, Shijingshan District, Beijing 100049, China*<sup>3</sup>*Key Laboratory of Radio Astronomy, Chinese Academy of Sciences, 20A Yuanhua Road, Nanjing, JiangSu 210033, China*<sup>4</sup>*National Astronomical Observatories, Chinese Academy of Sciences, 20A Datun Road, Chaoyang District, Beijing 100101, China*<sup>5</sup>*CAS Key Laboratory of FAST, National Astronomical Observatories, Chinese Academy of Sciences, Beijing 100101, China*<sup>6</sup>*National Radio Astronomy Observatory, Charlottesville, VA 22903, USA*<sup>7</sup>*Department of Physics and Astronomy, West Virginia University, Morgantown, WV 26506, USA*<sup>8</sup>*Center for Gravitational Waves and Cosmology, West Virginia University, Chestnut Ridge Research Building, Morgantown, WV 26505, USA*<sup>9</sup>*National Time Service Center, Chinese Academy of Sciences, Xi'an 710600, China*

## ABSTRACT

We report the discovery of the first radio pulsar associated with NGC 6712, an eclipsing black widow (BW) pulsar, J1853–0842A, found by high-sensitivity searches using the Five-hundred-meter Aperture Spherical radio Telescope. This 2.15 ms pulsar is in a 3.56 hr compact circular orbit with a very low mass companion likely of mass 0.018 to 0.036  $M_{\odot}$  and exhibits eclipsing of the pulsar signal. Though the distance to PSR J1853–0842A predicted from its dispersion measure ( $155.125 \pm 0.004 \text{ cm}^{-3} \text{ pc}$ ) and Galactic free electron density models are about 30% smaller than that of NGC 6712 obtained from interstellar reddening measurements, this is likely due to limited knowledge about the spiral arms and Scutum stellar cloud in this direction. Follow-up timing observations spanning 445 days allow us to localize the pulsar's position to be 0.14 core radii from the center of NGC 6712 and measure a negative spin-down rate for this pulsar of  $-2.39(2) \times 10^{-21} \text{ s s}^{-1}$ . The latter cannot be explained without the acceleration of the GC and decisively supports the association between PSR J1853–0842A and NGC 6712. Considering the maximum GC acceleration, Galactic acceleration, and Shklovskii effect, we place an upper limit on the intrinsic spin-down rate to be  $1.11 \times 10^{-20} \text{ s s}^{-1}$ . From an analysis of the eclipsing observations, we estimate the electron density of the eclipse region to be about  $1.88 \times 10^6 \text{ cm}^{-3}$ . We also place an upper limit of the accretion rate from the companion is about  $3.05 \times 10^{-13} M_{\odot} \text{ yr}^{-1}$  which is comparable with some other BWs.

**Keywords:** globular clusters: individual (NGC 6712) – pulsars: individual ( J1853–0842A)

## 1. INTRODUCTION

Globular Clusters (GCs) are tightly bound by gravity, giving them spherical shapes and relatively high stellar densities toward their centers. This environment provides a high specific incidence of low-mass X-ray binaries (LMXBs), the proposed progenitors of millisecond pulsars (MSPs), which enhances the possibility of finding new pulsars in GCs compared to the Galactic disk (see, e.g. Pooley et al. 2003; Ransom 2008). Since the discovery of first pulsar in M 28 (Lyne et al. 1987), there are currently about 217 pulsars known to be associated with Galactic GCs; most of these are binary MSPs (Freire 2013)<sup>1</sup>. In the core of a GC, more frequent interactions between stars take place as the stellar densities get even higher. The stellar interactions also produce exotic MSP binaries which are extremely rare in other places. The MSP is thought to have been spun up by the transfer of matter and angular momentum from its low-mass companion star during an X-ray-emitting phase. When a neutron star has been spun-up to millisecond periods,

Corresponding author: Zhen Yan  
yanzhen@shao.ac.cn

<sup>1</sup> <http://www3.mpifr-bonn.mpg.de/staff/pfreire/GCpsr.html>

**Table 1.** Observed properties of NGC 6712

Name	NGC 6712
Right Ascension (J2000)	18 <sup>h</sup> 53 <sup>m</sup> 04.3 <sup>s</sup>
Declination (J2000)	−08°42′22.0″
Galactic longitude, $l$ , (deg)	25.35
Galactic latitude, $b$ , (deg)	−4.32
Distance, $D$ , (kpc)	6.9
Core radius, $r_c$ , (arcmin)	0.76
Half-light radius, $r_h$ , (arcmin)	1.33
Central velocity dispersion, $\sigma_v$ (km/s)	4.3

its strong radiation has a possibility to quench accretion by ablating surrounding plasma, potentially evaporating the companion entirely to form an isolate MSP (Ruderman et al. 1989). Support for this scenario is provided by discoveries of eclipsing redback (RB) (Archibald et al. 2009) and black widow (BW) pulsars (Fruchter et al. 1988). These systems typically have compact orbits with periods shorter than 24 hr and are accompanied by low-mass companions with typical masses a few tenths of a solar mass or less ( $< 0.1 M_\odot$  for BWs and  $0.2 - 0.4 M_\odot$  for RBs). Evolutionary studies of BWs and RBs can provide important links between LMXBs and MSPs (Roberts 2013).

According to the catalog of GCs in the Milky Way, NGC 6712 is a metal-rich GC located about 6.9 kpc away from the Sun. The core and half-light radii of NGC 6712 are 0.76 and 1.33 arcmin, respectively. In Table 1, we list useful properties of NGC 6712 relate to this work obtained from the catalog<sup>2</sup> of GCs (Harris 1996). The stellar encounter rate for a GC can be estimated with  $\Gamma \propto \rho_c^{1.5} r_c^2$ , where  $\rho_c$  and  $r_c$  is the density and radius of the cluster core, respectively (Verbunt & Hut 1987). For NGC 6712,  $\Gamma$  is less than 1% of Terzan 5, where 39 pulsars have been discovered. In NGC 6712, there is a LMXB with the orbital period ( $P_b$ ) of 0.33 hr detected with the Einstein Observatory’s Monitor Proportional Counter (Leahy et al. 1983). In spite of a number of radio pulsar searches in NGC 6712 previously carried out, prior to this work, no pulsars were known in this cluster. This led to upper limits on pulsed emission of 11 mJy at 400 MHz (Biggs & Lyne 1996) and 16  $\mu$ Jy at 2.0 GHz (Lynch et al. 2011). Using scaling laws derived in previous population studies, which show that  $\Gamma$  is a strong indicator of pulsar abundance in GCs (Hui et al. 2010; Turk & Lorimer 2013), we estimate the population of pulsars in NGC 6712 to be  $\sim 5$  — much smaller than Terzan 5 and highlighting the importance of sensitive surveys such as the work described in this paper.

The Five-hundred-meter Aperture Spherical radio Telescope (FAST) is the largest single dish radio telescope in the world (Nan 2006). Benefiting from its 300-m illuminated aperture and low-noise cryogenic receivers, FAST can perform unprecedented high-sensitivity observations (Jiang et al. 2019). In this paper, we will present pulsar search results of NGC 6712 with FAST which have led to the discovery of the first pulsar in this cluster, PSR J1853–0842A. The rest of this paper is structured as follows: in Section 2, we describe the observations and data reduction procedures; in Section 3, we present the results of the search and follow-up timing observations; in Section 4, we discuss the implications and significance of our results.

## 2. OBSERVATIONS AND DATA REDUCTION

Observations of NGC 6712 were carried out with FAST using the central beam of the 19-beam L-band receiver (Jiang et al. 2020). For these observations, where the typical system temperature is about 20 K, the unparalleled gain of FAST leads to a system equivalent flux density of about 2 Jy, at least a factor of three improvement over the previous observations mentioned above. To carry out a dispersion measure (DM) search, the total bandwidth (1.05–1.45 GHz) was divided into sub-channels of 0.12 MHz and the data were acquired using the pulsar searching mode with a time resolution of 49.152  $\mu$ s. Following our discovery of the pulsar in the initial 30-min observation carried out on 2019 June 25 (MJD 58659), confirmation and follow-up observations were arranged on MJDs 58685 (observation length  $T_o = 120$  min,  $T_o$  will be omitted hereafter), 58686 (60 min), 58687 (30 min), 58768 (30 min), 58769 (30 min), 58931 (60 min), 58933 (60 min), 58963 (10 min), 58965 (10 min), and 59105 (30 min).

<sup>2</sup> <http://physwww.mcmaster.ca/~harris/mwgc.dat>

All data were searched for the presence of periodic dispersed pulses using **PRESTO**<sup>3</sup> (PulsAR Exploration and Search TOolkit) (Ransom 2011). Within **PRESTO**, the routine **rfifind** was used to mask and zap radio-frequency interference in both the time and frequency domains. The predicted DM of NGC 6712 is about  $182 \text{ cm}^{-3} \text{ pc}$  based on its distance (6.9 kpc) (Harris 1996) and the YMW16 Galactic free electron density models (Yao et al. 2017). As no pulsar was discovered in NGC 6712 previously, we searched for periodic signals in a DM range  $0\text{--}300 \text{ pc cm}^{-3}$  with the step of  $0.05 \text{ pc cm}^{-3}$ . The **PRESTO** routine **accelsearch** was used to analyse the data using a Fourier-domain acceleration search technique (Ransom et al. 2002) which, for a spin frequency  $f$  and an observation length  $T$ , was sensitive to frequency drifts  $z = \dot{f}T^2$  of up to  $z_{\text{max}} = 200$  Fourier bins. To search for even more highly accelerated binary systems, we also used the so-called “jerk search” technique (Andersen & Ransom 2018) which looks for signal drifts  $w = \dot{z} = \ddot{f}T^3$ . In our searches, we set the maximum drift  $w_{\text{max}} = 600$  bins. The python script **ACCEL\_sift.py** was used to produce a winnowed list of pulsar candidates from the searches. Beside the periodic pulse signal, we also used **single\_pulse\_search.py** to search for single pulses by setting the threshold to be 5.0.

### 3. RESULTS

We found a promising pulsar candidate with a spin period  $P = 2.149 \text{ ms}$  and DM of  $155.13 \text{ cm}^{-3} \text{ pc}$  in the initial observation from MJD 58659. With jerk search, the signal-to-noise ratios (SNR) of candidate detection was enhanced from 44.06 to 45.97. The signal was subsequently re-detected in follow-up observations with a SNR in the range 20.26–48.39. Each detection of the pulsar was further refined using the **PRESTO** routine **prepfold** which searched the data in period and DM to produce integrated pulse profiles with sub-integration lengths of 1.2 min. These period searches provided  $P$  and  $\dot{P}$  measurements for each observations which were then used to obtain a preliminary estimate of the orbital parameters of the pulsar using the analysis technique described by Freire et al. (2001). This initial spin and orbital ephemeris was subsequently supplied as input to the **TEMPO**<sup>4</sup> software package (Nice et al. 2015) which we used to carry out a full phase-coherent timing analysis of the time-of-arrival (TOA) for each folded profile. We used the **get\_toa.py** routine in **PRESTO** (which is an implementation of Fourier-domain template matching; Taylor 1992) to obtain TOAs which were analyzed in **TEMPO** using well-established methods (Lorimer & Kramer 2004).

The timing analysis resulted in a phase-coherent solution for the new pulsar, which we henceforth refer to as PSR J1853–0842A, over the MJD range 58659–59105. The timing residuals as a function of MJD, TOA number and orbital phase are presented in Fig. 1. The measured and derived parameters of PSR J1853–0842A are listed in the Table 2. As seen in Fig. 1, the extra time delays take place on three separate days, all of which correspond to the same orbital phase range (0.22–0.32). These phenomena should be caused by the eclipse of ionized material surrounding the companion star, as dispersion time delay was detected if we divided the total bandwidth into two sub-bands with the central frequency of 1.15 and 1.35 GHz respectively. The emission from the MSP is ablating its companion in such a narrow binary orbit. The expected geometry of this system should the eclipsing material be spherically symmetric and centered in the orbital plane at the distance of the companion. The maximum extra time delay is detected when the companion passes closest to our line of sight towards the pulsar (Polzin et al. 2019).

In Fig. 2, we present two samples of phase-time and integrated profile plots for PSR J1853–0842A based on the observations from MJD 58685 and 58768. The sub-integration time for the phase-time plots is about 7 min. Obvious time delays caused by eclipse are detected around 4900 s in the phase-time plot of observation on MJD 58685. The integrated profile of PSR J1853–0842A shows a simple structure with only a single peak. The widths at 50% and 10% of the peak of the integrated profile are  $W_{50} = 26.04 \pm 1.24^\circ$  and  $W_{10} = 63.41 \pm 2.56^\circ$ , respectively.

Since there were no radio flux density calibrators arranged in our observations, we estimate the flux density of PSR J1853–0842A using radiometer noise calculations (see, e.g., Lynch et al. 2011) which gives the off-pulse root-mean-square noise,

$$\sigma = \frac{T_{\text{sys}}}{G\sqrt{N_p\Delta\nu T_o}}. \quad (1)$$

Here  $T_{\text{sys}}$ ,  $G$ ,  $N_p$ ,  $\Delta\nu$ , and  $T_o$  are the system noise temperature, antenna gain, number of polarization, bandwidth and length of observation, respectively. Using the nominal values for these parameters, and adopting  $G = 11.3 \text{ K Jy}^{-1}$  (Jiang et al. 2019), since the zenith angle is large in our observations, we find the estimated mean flux density of PSR J1853–0842A to be  $16.1 \pm 2.9 \mu\text{Jy}$  at 1.25 GHz.

<sup>3</sup> <https://www.cv.nrao.edu/~sransom/presto>

<sup>4</sup> <http://tempo.sourceforge.net>

**Table 2.** Observed and derived parameters of PSR J1853–0842A

Pulsar	J1853–0842A
Right Ascension, $\alpha$ (J2000)	18 <sup>h</sup> 53 <sup>m</sup> 04.07409(2) <sup>s</sup>
Declination, $\delta$ (J2000)	−08°42′28.254(2)″
Spin Frequency, $f_0$ (s <sup>−1</sup> )	465.23897161363(7)
1 <sup>st</sup> Spin Frequency derivative, $f_1$ (Hz s <sup>−2</sup> )	5.18(4)×10 <sup>−16</sup>
Reference Epoch (MJD)	58685.702931
Start of Timing Data (MJD)	58659.715
End of Timing Data (MJD)	59105.545
Dispersion Measure, DM (pc cm <sup>−3</sup> )	155.125(4)
Solar System Ephemeris	DE200
Number of TOAs	344
Residuals RMS ( $\mu$ s)	3.77
Binary Parameters	
Binary Model	BT
Projected Semi-major Axis, $x_p$ (lt-s)	4.91856(2)×10 <sup>−2</sup>
Orbital Eccentricity, $e$	0.00
Longitude of Periastron, $\omega$ (deg)	0.00
Epoch of passage at Periastron, $T_0$ (MJD)	58685.64161943(9)
Orbital Period, $P_b$ (days)	0.1482829972(2)
Derived Parameters	
Spin Period, $P$ (s)	2.1494330032835(3)×10 <sup>−3</sup>
1 <sup>st</sup> Spin Period derivative, $\dot{P}$ (s s <sup>−1</sup> )	−2.39(2)×10 <sup>−21</sup>
Distance based on TC93 <sup>a</sup> , $D_{TC93}$ (kpc)	4.55
Distance based on NE2001 <sup>b</sup> , $D_{NE2001}$ (kpc)	3.79
Distance based on YMW16 <sup>c</sup> , $D_{YMW16}$ (kpc)	4.76
Mass function, $f(M_p, M_c)$ ( $M_\odot$ )	5.81 × 10 <sup>−6</sup>
Possible range of $M_c$ <sup>d</sup> ( $M_\odot$ ),	0.018 ≤ $M_c$ ≤ 0.036

<sup>a</sup> Taylor & Cordes (1993)<sup>b</sup> Cordes & Lazio (2002)<sup>c</sup> Yao et al. (2017)<sup>d</sup> For  $i \geq 60.0^\circ$  and  $1.0 M_\odot \leq M_p \leq 2.2 M_\odot$  (see Sect. 4)

#### 4. DISCUSSION

Beside the 6.9 kpc adopted in the Galactic GC catalog (Harris 1996), there are some other distance results of NGC 6712, e.g. 6.75 kpc (Sandage & Smith 1966), 6.2 kpc (Webbink 1985), 7.9 kpc (Ortolani et al. 2000), which were also obtained base on interstellar reddening measurements. Overall, DM-based distances of PSR J1853–0842A listed in Table 1 are much smaller than previous distance results of NGC 6712. Normally, distance results obtained with interstellar reddening measurements are comparatively reliable, as they are supported by model-independent parallax measurements on a large sample of stars at optical band (Fuhrmann 2004). By comparison, only 144 pulsars’ distances are obtained with parallax measurements<sup>5</sup>. To give further estimate on whether PSR J1853–0842A is in NGC 6712 or not. We firstly did an assessment about the validation of distance based on the Galactic electron density models along this direction. Comparisons of model-independent distances of about 50 pulsars obtained with the Very Long Baseline Array (VLBA) to those predicted by the NE2001 (Cordes & Lazio 2002) and YMW16 (Yao et al. 2017) Galactic electron density distribution models show that it is hard to give definite conclusion on which model is more accurate. Both models show large errors for some objects, with the NE2001 model doing better on some objects and the YMW16

<sup>5</sup> <http://hosting.astro.cornell.edu/~shami/psrvlb/parallax.html>

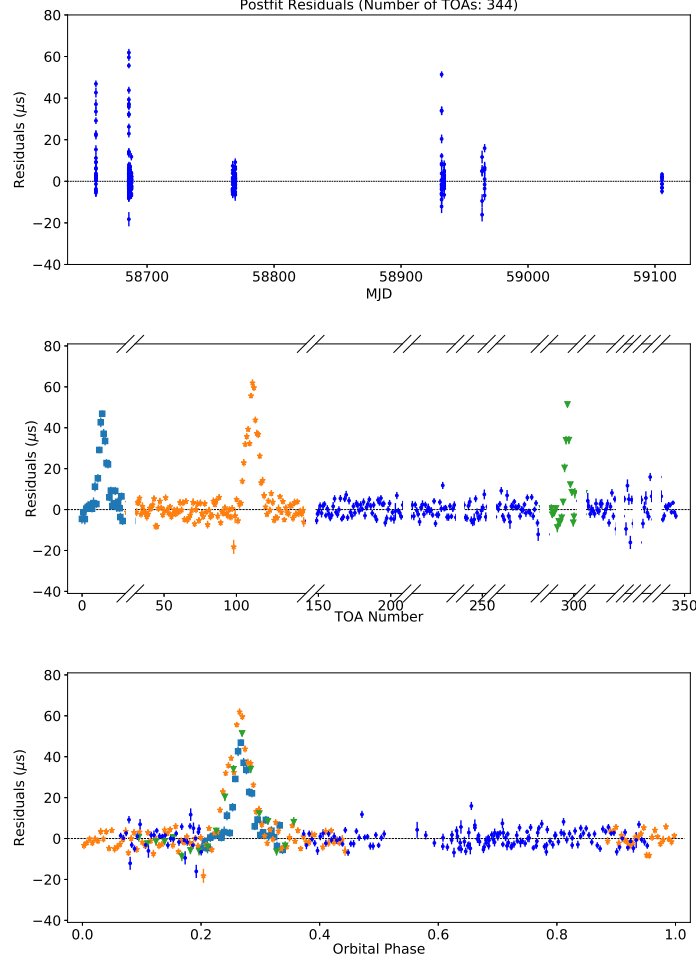


**Figure 1.** Timing residuals for PSR J1853–0842A as a function of MJD (top), time-of-arrival (TOA) number (middle), and orbital phase (bottom). The cyan squares, orange stars and green triangles in the plot shown in the middle and bottom panels are corresponding to the observation results on MJD 58659, 58685 and 58931, respectively. Pulsar eclipses were detected on each of these days. In the middle panel, observation results from different epochs are separated by breaks on the horizontal axes of the plot. The integration length of each point is about 1.2 min.

model on others. For about 14% of those 50 pulsars, their distances based on the YMW16 model fall outside the range of 0.1 to 1.9 times of corresponding real results obtained with the VLBA (Deller et al. 2019). The Galactic longitude and latitude of NGC 6712 is  $25.35^\circ$  and  $-4.32^\circ$ , respectively. We have limited information about spiral arms and Scutum stellar cloud along this direction. There is only one pulsar that has model-independent distance measurement result within  $5^\circ$  around NGC 6712. As we do not know which Galactic electron density model is more accurate, we give a statistic on  $D_{\text{YMW16}}$  and  $D_{\text{NE2001}}$  of 87 pulsars within  $5^\circ$  around NGC 6712. The distances of these pulsars are obtained from pulsar catalog (PSRCAT) (Manchester et al. 2005)<sup>6</sup>. Fig. 3 shows the  $D_{\text{YMW16}}/D_{\text{NE2001}}$  ratios of these 87 pulsars change with  $D_{\text{YMW16}}$ . It is clear the ratio gets larger as the  $D_{\text{YMW16}}$  gets further. When the  $D_{\text{YMW16}}$  is larger than 6.0 kpc, the ratio can get as large as more than 2.5 times. So, the association between PSR J1853–0842A and NGC 6712 can not simply be excluded base on their large model-dependent distance differences mentioned above because of their unknown accuracy.

The rotation of a pulsar usually slows down with time, as its rotational energy is converted to radiation power. So, the intrinsic spin-down rate ( $\dot{P}_{\text{int}}$ ) ought to be a positive value. But, the observed spin-down rate ( $\dot{P}_{\text{obs}}$ ) of PSR J1853–0842A is about  $-2.39 \times 10^{-21} \text{ s s}^{-1}$ , which is a negative result. The  $\dot{P}_{\text{int}}$  of a pulsar (especially MSP) is

<sup>6</sup> <http://www.atnf.csiro.au/research/pulsar/psrcat>

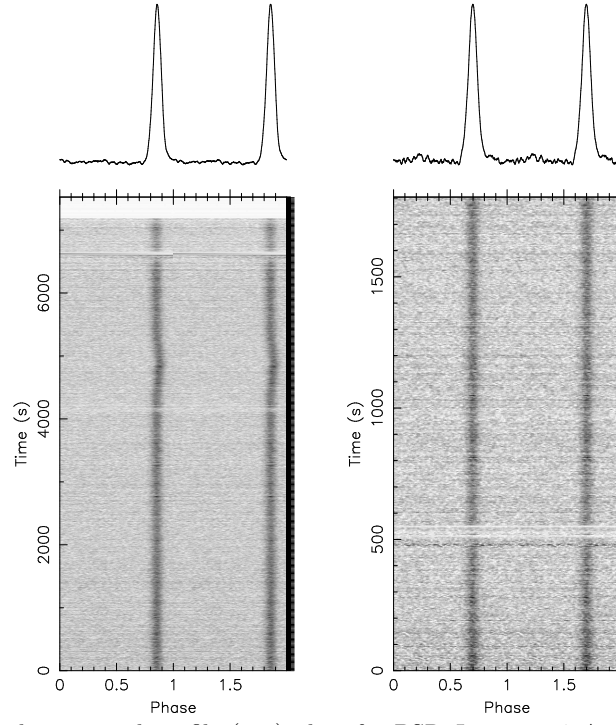


**Figure 2.** Phase-time (bottom) and integrated profile (top) plots for PSR J1853–0842A obtained with observation data on MJD 58685 (left) and 58768 (right).

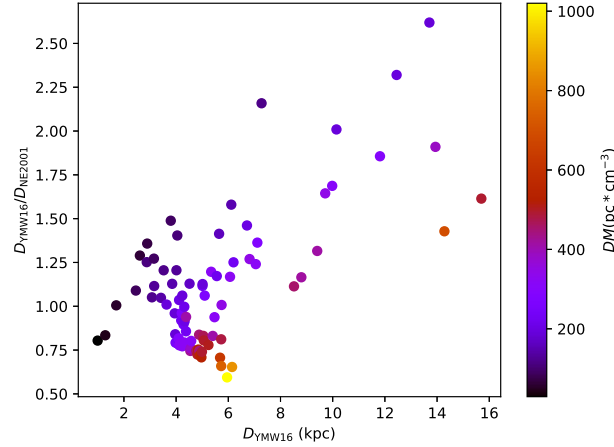


**Figure 3.**  $D_{\text{YMW16}}/D_{\text{NE2001}}$  changes with  $D_{\text{YMW16}}$  for 87 pulsars within  $5^\circ$  around NGC 6712. The DM value of each pulsar is scaled with the color bar on the right.

usually contaminated by acceleration of the host Galaxy ( $a_G$ ) and the Shklovskii effect caused by its proper motion (Shklovskii 1970). In addition, the acceleration effect of the host GC ( $a_L$ ) should also be considered as it sometimes gives **the dominant** contribution to the  $\dot{P}_{\text{obs}}$  of the pulsar in the GC. According to Phinney (1993),

$$\dot{P}_{\text{obs}} = \dot{P}_{\text{int}} + \frac{a_G}{c}P + \frac{V_\perp^2}{cD}P + \frac{a_L}{c}P, \quad (2)$$

where  $P$  is the observed pulsar period,  $V_\perp^2/cD$  is the Shklovskii effect,  $V_\perp$  is the transverse velocity,  $D$  is the distance to the pulsar, and  $c$  is the speed of light. We assume the Galaxy has a flat rotation curve in the region of interest, with the Galactocentric distance of the Sun  $R_0 = 8.0$  kpc and rotation velocity  $\Theta = 220$  km s $^{-1}$  (Reid 1993). A



straightforward geometric analysis gives the line-of-sight acceleration between the Sun and a pulsar at distance  $D$  and Galactic **coordinates**  $l$  and  $b$  as follows:

$$a_G = -\cos b \left( \frac{\Theta_0}{R_0} \right) \left( \cos l + \frac{\beta}{\sin^2 l + \beta^2} \right), \quad (3)$$

where  $\beta = (D/R_0) \cos b - \cos l$  (Damour & Taylor 1991). In the Shklovskii effect calculation, we use  $V_\perp = 85 \text{ km s}^{-1}$  which is the average velocity of MSPs (Toscano et al. 1999), as the velocity of PSR J1853–0842A was not be fitted successfully with our observation data. If PSR J1853–0842A lies outside the NGC 6712 at a distance of 4.4 kpc (the average DM-based distances list in Table 2), the  $a_G/(cP)$  and  $V_\perp^2 P/(cD)$  is  $3.81 \times 10^{-22}$  and  $3.42 \times 10^{-22} \text{ s s}^{-1}$ , respectively. Taking  $\dot{P}_{\text{int}} > 0$  and  $a_L/cP = 0$  into consideration, it is impossible to obtained  $\dot{P}_{\text{obs}} = -2.39 \times 10^{-21}$  as all the terms on the right of Eq. 2 are no less than 0. On the other hand, if PSR J1853–0842A is located in NGC 6712 at the distance of 6.9 kpc,  $a_G/(cP)$  and  $V_\perp^2 P/(cD)$  is  $2.43 \times 10^{-22}$  and  $-9.35 \times 10^{-22} \text{ s s}^{-1}$  respectively with the same assumption  $V_\perp = 85 \text{ km s}^{-1}$ . Compared the core position of NGC 6712 and PSR J1853–0842A listed in Table 1 and 2, it is clear that the pulsar’s projected distance from the center of the GC ( $R_{\text{psr}}$ ) is less than two times of its core radius ( $R_c$ ). Under this condition, the maximum accelerations effect of GC can be estimated within 10% of accuracy with the equations:

$$\frac{a_{L,\text{max}}}{c} \approx \frac{3\sigma_v^2}{2c(R_c^2 + R_{\text{psr}}^2)^{1/2}} \quad (4)$$

where  $\sigma_v$  is the central velocity dispersion (Phinney 1993). For PSR J1853–0842A, the  $a_{L,\text{max}}/cP$  is about  $1.28 \times 10^{-20} \text{ s s}^{-1}$ . Though we do not know three-dimensional position of PSR J1853–0842A in NGC 6712 at present, its real  $a_L/cP$  is a certain value in the range of  $-1.28 \times 10^{-20}$  to  $1.28 \times 10^{-20} \text{ s s}^{-1}$ . Accordingly, we give an upper limit of its intrinsic spin-down rate  $\dot{P}_{\text{int,max}} = 1.11 \times 10^{-20} \text{ s s}^{-1}$ . It is a reasonable value judging the  $\dot{P}$  measure results of some other BWs. Taking PSRs B1957+20 and J2051–0827 for example, their  $\dot{P}$  is  $2.7 \times 10^{-20}$  and  $1.27 \times 10^{-20} \text{ s s}^{-1}$ , respectively (Arzoumanian et al. 1994; Shaifullah et al. 2016).

Using the orbital period  $P_b$  and the projected semi-major axis  $x_p$  of the pulsar orbit, the mass function

$$f(M_p, M_c) = \frac{4\pi^2}{G} \frac{x_p^3}{P_b^2} = \frac{(M_c \sin i)^3}{(M_p + M_c)^2}, \quad (5)$$

where  $G$  is the gravitational constant,  $M_p$  is the mass of the pulsar,  $M_c$  is the mass of companion star, and  $i$  is the inclination of the binary orbit. Though PSR J1853–0842A is a short  $P_b$  binary, it is very hard to determine the mass of each star by measuring post-Keplerian parameters with pulsar timing because of its weak general relativity effects. As the  $M_p$  and  $i$  of this binary can not be measured with our observation data, we estimate  $M_c$  under some assumptions. According to previous studies, the mass of a radio pulsar predominantly falls a remarkably narrow mass range  $1.38_{-0.10}^{+0.06} M_\odot$  (Thorsett & Chakrabarty 1999). The canonical value of a pulsar  $1.4 M_\odot$  is usually used in most cases. But, there are some exceptions, such as PSR J1918-0642 with extremely low mass of  $1.18 M_\odot$  (Fonseca et al. 2016) and PSR J0740+6620 with extremely high mass of  $2.14 M_\odot$  (Cromartie et al. 2020). Taking these into consideration, further limitations on the  $M_c$  are given by assuming the  $M_p$  to be 1.0, 1.4, and  $2.2 M_\odot$ , respectively. The curves of  $M_c$  changing with  $i$  and  $M_p$  are presented in Fig. 4. As the eclipse takes place in PSR J1853–0842A, its inclination angle  $i$  must be greater than  $60^\circ$ . We calculate  $M_{c,60^\circ}$  for the different assumption of the  $M_p$  and listed related results in the 2nd column of Table 3. Lower limits of the companion mass ( $M_{c,90^\circ}$ ) are obtained by assuming an edge-on orbit ( $i = 90^\circ$ ). The corresponding results of  $M_{c,90^\circ}$  values are present in the 3rd column of Table 3. The Roche lobe for the companion star of PSR J1853–0842A is calculated by the equation:

$$R_L = \frac{0.49aq^{2/3}}{0.6q^{2/3} + \ln(1 + q^{1/3})}, \quad (6)$$

where  $q = M_c/M_p$  and  $a$  is the separation between the pulsar and its companion (Eggleton 1983). The related results for different  $M_p$  and  $i$  are present in the 4th (for  $i = 60^\circ$ ) and 5th (for  $i = 90^\circ$ ) column of Table 3.

About half of known BW pulsars show eclipse phenomena in which the radio pulses are completely blocked by companion stars (Guillemot et al. 2019). By comparison, the pulse signals of PSR J1853–0842A are affected by extra time delay, but not absolutely blocked during eclipse phase. Base on the extra time delay lasted for about 10% of its orbit at 1.25 GHz, we estimate the radius of ionized material surrounding its companion star ( $R_e$ ) for different orbital

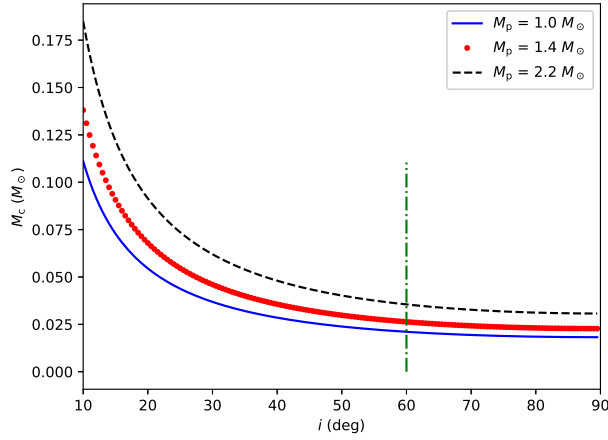


**Figure 4.** The  $M_c$  as a function of  $i$  and  $M_p$ . The case for the assumption  $M_p = 1.0 M_\odot$ ,  $M_p = 1.4 M_\odot$ , and  $M_p = 2.2 M_\odot$  is shown with solid, dotted and dash curve, respectively. The dash-dot vertical line stands for  $i = 60^\circ$

**Table 3.** The results of  $M_c$ ,  $R_L$ ,  $R_e$  for different  $i$  and  $M_p$

$M_p$ ( $M_\odot$ )	$M_c$ ( $M_\odot$ )		$R_L$ ( $R_\odot$ )		$R_e$ ( $R_\odot$ )	
	$M_{c,60^\circ}$	$M_{c,90^\circ}$	$R_{L,60^\circ}$	$R_{L,90^\circ}$	$R_{e,60^\circ}$	$R_{e,90^\circ}$
1.0	0.021	0.018	0.140	0.134	0.381	0.330
1.4	0.026	0.023	0.152	0.145	0.427	0.370
2.2	0.036	0.031	0.168	0.160	0.497	0.430

inclination angle and give the related results in the 6th (for  $i = 60^\circ$ ) and 7th (for  $i = 90^\circ$ ) column of Table 3. It is clear that the  $R_L$  is smaller than  $R_e$ , which indicates that ionized material fully fills the Roche lobe of the companion star. So, the outer material is being blown off the companion by the pulsar. As what is shown in this table, the  $M_c$ ,  $R_L$  and  $R_e$  is within a factor of 2.0, 1.3 and 1.5 of the minimum values, respectively. So, we will use the values corresponding to the case of canonical pulsar mass  $M_p = 1.4 M_\odot$  and  $i = 90^\circ$  in the following estimation about the properties of eclipse material.

Using the extra delays shown in the timing residual plot in Fig. 1, we obtain the corresponding maximum excess dispersion measure ( $\Delta_{DM}$ ), which was about  $0.028 \pm 0.001$ ,  $0.036 \pm 0.001$ , and  $0.030 \pm 0.002$  pc cm $^{-3}$ , respectively. The column density of electron ( $N_{e,max}$ ) in the eclipse material was about  $9.69 \times 10^{16}$  cm $^{-2}$  estimated with the average  $\Delta_{DM}$ , which is about 5.7 times larger than that of BW PSR J0023-7203J ( $N_{e,max} = 1.7 \times 10^{16}$  cm $^{-2}$ ). The radiations of PSR J0023-7203J also passed the material around companion at both 660 and 1400 MHz with extra time delays (Freire et al. 2003). The radiations of several BWs are blocked at low radio frequencies, but get passed at higher frequencies with extra time delays. PSR J1544+4937 was found to be eclipsing for 13% of its orbit at 322 MHz, whereas the pulsar was detected throughout the low-frequency eclipsing phase at 607 MHz, which was affected by the material around its companion with  $N_{e,max} = 8 \times 10^{16}$  cm $^{-2}$  (Bhattacharyya et al. 2013). The material with  $N_{e,max} \sim 10^{17}$  cm $^{-2}$  surrounding BW PSR J2051-0827's companion was also found to be opaque for radiations at 436 and 660 MHz, but transparent at 1.4 GHz (Stappers et al. 1996). By comparison, the  $N_{e,max}$  near the superior conjunction of BW PSR J2055+3829 was no less than  $10^{17}$  cm $^{-2}$ , which was larger than that of BWs mentioned above. And, its radiation was found to be blocked at 1.4 GHz in eclipse phase (Guillemot et al. 2019). Judging from the information mentioned above, we infer that radiation PSR J1853-0842A has possibilities to be blocked at lower radio frequencies.

Graduate flux density decreases (and increase) were detected in PSRs J2051-0827 and J2055+3829 before (and after) their radiations were completely eclipsed at the corresponding frequency (Stappers et al. 1996; Guillemot et al. 2019). For PSR J1853-0842A, we also analyzed on its pulse flux density and shape changes with time to investigate how they changed in the eclipse phase. Considering the sensitivity and the time resolution, the  $W_{50}$  were used in



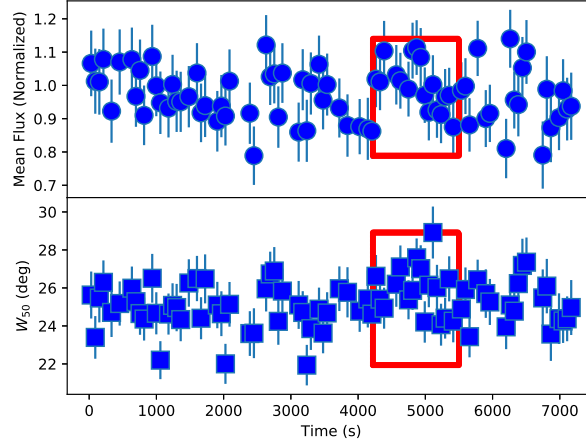


**Figure 5.** The  $W_{50}$  and normalized flux density changed with time for observation on MJD 58685. The eclipse time range is labeled with the red box.

the pulse shape analysis, and the mean flux normalized with the peak flux density of integrated profile were used to seek its flux variations. Fig 5 shows how these two parameters changed in observation on MJD 58685, which spanned longest time and covered the full eclipse phase. No clear change in flux density and  $W_{50}$  were found in the eclipse phase compared with normal state.

Base on the eclipse properties of PSR J1853–0842A, we try to give some constrains on the accretion process of this system. From the results listed in Table 3, it is clear that  $R_e$  does not change a lot for different assumptions of  $i$  and  $M_p$ . Considering only upper limit of  $\dot{P}_{\text{int,max}}$  obtained and eclipse-to-eclipse variability of extra DM delays, we only give rough estimations on the accretion with the average volume density of electron  $n_e = 1.88 \times 10^6 \text{ cm}^{-3}$  by assuming  $M_p = 1.4M_\odot$  and  $i = 90^\circ$ . The energy density of an isotropic pulsar wind at the distance of the companion is given by  $U_E = \dot{E}/(4\pi ca^2)$ , where  $\dot{E} = 4\pi^2 I \dot{P} P^{-3}$  is the spin-down power of the pulsar,  $I$  is the moment of inertia and  $a$  is the distance to the companion. For the canonical  $1.4 M_\odot$  neutron star of radius 10 km and moment of inertia  $I = 10^{45} \text{ g cm}^2$ , the maximum  $\dot{E}$  of PSR J1853–0842A is about  $4.42 \times 10^{34} \text{ erg s}^{-1}$ . If the pulsar wind energy flow is converted into a mass outflow of kinetic energy density with an efficiency factor  $\epsilon$ , the outflow velocity of ablated material from the companion star,

$$V_W \approx \left( \frac{2\epsilon U_E}{n_e m_p} \right)^{1/2}, \quad (7)$$

where  $n_e$  and  $m_p$  is the electron column density and proton mass, respectively (Thompson et al. 1994). By assuming  $\epsilon = 1$ , the upper limit of mass loss rate from the companion  $\dot{M}_C \simeq \pi R_e m_p n_e V_W$ . For PSR J1853–0842A, the corresponding upper limit of  $\dot{M}_C$  should be about  $3.05 \times 10^{-13} M_\odot \text{ yr}^{-1}$ . By comparison, the  $\dot{M}_C$  of PSR J1810+1744 is  $6 \times 10^{-13} M_\odot \text{ yr}^{-1}$  and  $1 \times 10^{-12} M_\odot \text{ yr}^{-1}$  obtained block information at 149 MHz and 345 MHz, respectively (Polzin et al. 2018). The inferred accretion rates of these two BWs are comparable.

Overall, the newly-discovered BW pulsar J1853–0842A is most probably in NGC 6712. During the eclipse phase, its signals showed eclipse-to-eclipse varying extra time delays but were not blocked. The average  $N_{e,\text{max}}$  of material around J1853–0842A’s companion is about  $9.69 \times 10^{16} \text{ cm}^{-2}$ , which is a medium value compared with BWs that show only extra time delays and absolutely-blocked phenomena in the eclipse phase. Its inferred upper limit of  $\dot{M}_C$  is about  $3.05 \times 10^{-13} M_\odot \text{ yr}^{-1}$  is also comparable with some other BWs. We **predict** that the radiation of PSR J1853–0842A has the possibility to be blocked at lower radio frequencies, **and will test this hypothesis with future observations.**

#### ACKNOWLEDGMENTS

We would like to express our appreciations to the anonymous reviewer and Professor R. N. Manchester for their good suggestions. This work was supported in part by the National Natural Science Foundation of China (Grant Nos. U2031119, U1631122, 11633007, and 11403073), the Strategic Priority Research Program of the Chinese Academy of

Sciences (XDB23010200), the National Key R&D Program of China (2018YFA0404602) and the Knowledge Innovation Program of the Chinese Academy of Sciences (KJ CX1-YW-18). Five-hundred-meter Aperture Spherical radio Telescope (FAST) is a National Major Scientific Project built by the Chinese Academy of Sciences. Funding for the project has been provided by the National Development and Reform Commission. FAST is operated and managed by the National Astronomical Observatories, Chinese Academy of Sciences.

## REFERENCES

- Andersen, B. C., & Ransom, S. M. 2018, *ApJ*, 863, L13, doi: [10.3847/2041-8213/aad59f](https://doi.org/10.3847/2041-8213/aad59f)
- Archibald, A. M., Stairs, I. H., Ransom, S. M., et al. 2009, *Science*, 324, 1411, doi: [10.1126/science.1172740](https://doi.org/10.1126/science.1172740)
- Arzoumanian, Z., Fruchter, A. S., & Taylor, J. H. 1994, *ApJ*, 426, L85, doi: [10.1086/187346](https://doi.org/10.1086/187346)
- Bhattacharyya, B., Roy, J., Ray, P. S., et al. 2013, *ApJ*, 773, L12, doi: [10.1088/2041-8205/773/1/L12](https://doi.org/10.1088/2041-8205/773/1/L12)
- Biggs, J. D., & Lyne, A. G. 1996, *MNRAS*, 282, 691
- Cordes, J. M., & Lazio, T. J. W. 2002, arXiv e-prints, astro. <https://arxiv.org/abs/astro-ph/0207156>
- Cromartie, H. T., Fonseca, E., Ransom, S. M., et al. 2020, *Nature Astronomy*, 4, 72, doi: [10.1038/s41550-019-0880-2](https://doi.org/10.1038/s41550-019-0880-2)
- Damour, T., & Taylor, J. H. 1991, *ApJ*, 366, 501, doi: [10.1086/169585](https://doi.org/10.1086/169585)
- Deller, A. T., Goss, W. M., Briskin, W. F., et al. 2019, *ApJ*, 875, 100, doi: [10.3847/1538-4357/ab11c7](https://doi.org/10.3847/1538-4357/ab11c7)
- Eggleton, P. P. 1983, *ApJ*, 268, 368
- Fonseca, E., Pennucci, T. T., Ellis, J. A., et al. 2016, *ApJ*, 832, 167, doi: [10.3847/0004-637X/832/2/167](https://doi.org/10.3847/0004-637X/832/2/167)
- Freire, P. C., Camilo, F., Kramer, M., et al. 2003, *MNRAS*, 340, 1359, doi: [10.1046/j.1365-8711.2003.06392.x](https://doi.org/10.1046/j.1365-8711.2003.06392.x)
- Freire, P. C., Kramer, M., & Lyne, A. G. 2001, *MNRAS*, 322, 885
- Freire, P. C. C. 2013, in *IAU Symposium*, Vol. 291, *Neutron Stars and Pulsars: Challenges and Opportunities after 80 years*, ed. J. van Leeuwen, 243–250, doi: [10.1017/S1743921312023770](https://doi.org/10.1017/S1743921312023770)
- Fruchter, A. S., Stinebring, D. R., & Taylor, J. H. 1988, *Nature*, 333, 237, doi: [10.1038/333237a0](https://doi.org/10.1038/333237a0)
- Fuhrmann, K. 2004, *Astronomische Nachrichten*, 325, 3, doi: [10.1002/asna.200310173](https://doi.org/10.1002/asna.200310173)
- Guillemot, L., Octau, F., Cognard, I., et al. 2019, *A&A*, 629, A92, doi: [10.1051/0004-6361/201936015](https://doi.org/10.1051/0004-6361/201936015)
- Harris, W. E. 1996, *AJ*, 112, 1487
- Hui, C. Y., Cheng, K. S., & Taam, R. E. 2010, *ApJ*, 714, 1149, doi: [10.1088/0004-637X/714/2/1149](https://doi.org/10.1088/0004-637X/714/2/1149)
- Jiang, P., Yue, Y., Gan, H., et al. 2019, *Science China Physics, Mechanics, and Astronomy*, 62, 959502, doi: [10.1007/s11433-018-9376-1](https://doi.org/10.1007/s11433-018-9376-1)
- Jiang, P., Tang, N.-Y., Hou, L.-G., et al. 2020, *Research in Astronomy and Astrophysics*, 20, 064, doi: [10.1088/1674-4527/20/5/64](https://doi.org/10.1088/1674-4527/20/5/64)
- Leahy, D. A., Darbro, W., Elsner, R. F., et al. 1983, *ApJ*, 266, 160
- Lorimer, D. R., & Kramer, M. 2004, *Handbook of Pulsar Astronomy*, Vol. 4
- Lynch, R. S., Ransom, S. M., Freire, P. C. C., & Stairs, I. H. 2011, *ApJ*, 734, 89, doi: [10.1088/0004-637X/734/2/89](https://doi.org/10.1088/0004-637X/734/2/89)
- Lyne, A. G., Brinklow, A., Middleditch, J., et al. 1987, *Nature*, 328, 399
- Manchester, R. N., Hobbs, G. B., Teoh, A., & Hobbs, M. 2005, *AJ*, 129, 1993, doi: [10.1086/428488](https://doi.org/10.1086/428488)
- Nan, R. 2006, *Science in China: Physics, Mechanics and Astronomy*, 49, 129, doi: [10.1007/s11433-006-0129-9](https://doi.org/10.1007/s11433-006-0129-9)
- Nice, D., Demorest, P., Stairs, I., et al. 2015, *Tempo: Pulsar timing data analysis*. <http://ascl.net/1509.002>
- Ortolani, S., Momany, Y., Barbay, B., Bica, E., & Catelan, M. 2000, *A&A*, 362, 953
- Phinney, E. S. 1993, in *Astronomical Society of the Pacific Conference Series*, Vol. 50, *Structure and Dynamics of Globular Clusters*, ed. S. G. Djorgovski & G. Meylan, 141
- Polzin, E. J., Breton, R. P., Stappers, B. W., et al. 2019, *MNRAS*, 490, 889, doi: [10.1093/mnras/stz2579](https://doi.org/10.1093/mnras/stz2579)
- Polzin, E. J., Breton, R. P., Clarke, A. O., et al. 2018, *MNRAS*, 476, 1968, doi: [10.1093/mnras/sty349](https://doi.org/10.1093/mnras/sty349)
- Pooley, D., Lewin, W. H. G., Anderson, S. F., et al. 2003, *apjl*, 591, L131, doi: [10.1086/377074](https://doi.org/10.1086/377074)
- Ransom, S. 2011, *PRESTO: PulsAR Exploration and Search TOolkit*. <http://ascl.net/1107.017>
- Ransom, S. M. 2008, in *American Institute of Physics Conference Series*, Vol. 983, *40 Years of Pulsars: Millisecond Pulsars, Magnetars and More*, ed. C. Bassa, Z. Wang, A. Cumming, & V. M. Kaspi, 415–423, doi: [10.1063/1.2900267](https://doi.org/10.1063/1.2900267)
- Ransom, S. M., Eikenberry, S. S., & Middleditch, J. 2002, *AJ*, 124, 1788
- Reid, M. J. 1993, *ARA&A*, 31, 345, doi: [10.1146/annurev.aa.31.090193.002021](https://doi.org/10.1146/annurev.aa.31.090193.002021)

- Roberts, M. S. E. 2013, in IAU Symposium, Vol. 291, Neutron Stars and Pulsars: Challenges and Opportunities after 80 years, ed. J. van Leeuwen, 127–132, doi: [10.1017/S174392131202337X](https://doi.org/10.1017/S174392131202337X)
- Ruderman, M., Shaham, J., & Tavani, M. 1989, ApJ, 336, 507, doi: [10.1086/167029](https://doi.org/10.1086/167029)
- Sandage, A., & Smith, L. L. 1966, ApJ, 144, 886, doi: [10.1086/148686](https://doi.org/10.1086/148686)
- Shaifullah, G., Verbiest, J. P. W., Freire, P. C. C., et al. 2016, MNRAS, 462, 1029, doi: [10.1093/mnras/stw1737](https://doi.org/10.1093/mnras/stw1737)
- Shklovskii, I. S. 1970, Soviet Ast., 13, 562
- Stappers, B. W., Bailes, M., Lyne, A. G., et al. 1996, ApJ, 465, L119, doi: [10.1086/310148](https://doi.org/10.1086/310148)
- Taylor, J. H. 1992, Philosophical Transactions of the Royal Society of London Series A, 341, 117, doi: [10.1098/rsta.1992.0088](https://doi.org/10.1098/rsta.1992.0088)
- Taylor, J. H., & Cordes, J. M. 1993, ApJ, 411, 674, doi: [10.1086/172870](https://doi.org/10.1086/172870)
- Thompson, C., Blandford, R. D., Evans, C. R., & Phinney, E. S. 1994, ApJ, 422, 304, doi: [10.1086/173728](https://doi.org/10.1086/173728)
- Thorsett, S. E., & Chakrabarty, D. 1999, ApJ, 512, 288
- Toscano, M., Sandhu, J. S., Bailes, M., et al. 1999, MNRAS, 307, 925, doi: [10.1046/j.1365-8711.1999.02685.x](https://doi.org/10.1046/j.1365-8711.1999.02685.x)
- Turk, P. J., & Lorimer, D. R. 2013, MNRAS, 436, 3720, doi: [10.1093/mnras/stt1850](https://doi.org/10.1093/mnras/stt1850)
- Verbunt, F., & Hut, P. 1987, in The Origin and Evolution of Neutron Stars, IAU Symposium No. 125, ed. D. J. Helfand & J. Huang (Dordrecht: Reidel), 187–197
- Webbink, R. F. 1985, in IAU Symposium, Vol. 113, Dynamics of Star Clusters, ed. J. Goodman & P. Hut, 541–577
- Yao, J. M., Manchester, R. N., & Wang, N. 2017, ApJ, 835, 29, doi: [10.3847/1538-4357/835/1/29](https://doi.org/10.3847/1538-4357/835/1/29)